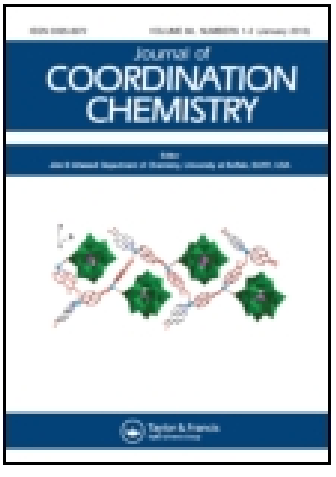

Journal of Coordination Chemistry
Publication details, including instructions for authors and subscription information:
http://www.tandfonline.com/loi/gcoo20

Co(III) and Fe(III) complexes of Schiff bases derived from 2,4-dihydroxybenzaldehyde S-allyl-isothiosemicarbazonehydrobromide

Reza Takjoo[a], Joel T. Mague[b], Alireza Akbari[c] & Mehdi Ahmadi[c]

[a] Department of Chemistry, School of Sciences, Ferdowsi University of Mashhad, Mashhad, Iran

[b] Department of Chemistry, Tulane University, New Orleans, LA, USA

[c] Department of Chemistry, Payame Noor University (PNU), Tehran, Iran

Accepted author version posted online: 18 Oct 2013.Published online: 26 Nov 2013.

To cite this article: Reza Takjoo, Joel T. Mague, Alireza Akbari & Mehdi Ahmadi (2013) Co(III) and Fe(III) complexes of Schiff bases derived from 2,4-dihydroxybenzaldehyde S-allyl-isothiosemicarbazonehydrobromide, Journal of Coordination Chemistry, 66:22, 3915-3925, DOI: 10.1080/00958972.2013.856420

To link to this article: http://dx.doi.org/10.1080/00958972.2013.856420

Journal of Coordination Chemistry, 2013
Vol. 66, No. 22, 3915–3925, http://dx.doi.org/10.1080/00958972.2013.856420

Co(III) and Fe(III) complexes of Schiff bases derived from 2,4-dihydroxybenzaldehyde *S*-allyl-isothiosemicarbazonehydrobromide

REZA TAKJOO*†, JOEL T. MAGUE‡, ALIREZA AKBARI§ and MEHDI AHMADI§

†Department of Chemistry, School of Sciences, Ferdowsi University of Mashhad, Mashhad, Iran
‡Department of Chemistry, Tulane University, New Orleans, LA, USA
§Department of Chemistry, Payame Noor University (PNU), Tehran, Iran

(*Received 21 October 2012; accepted 18 September 2013*)

Two new complexes, $[Co(L^1)(Py)_3]Cl_{0.75}Br_{0.25}$ (L^1=4-hydroxy salicylaldehyde *S*-allyl-isothiosemicarbazonato-N,N',O) and $[Fe(L^2)Cl]\cdot C_2H_5OH$ (L^2=*S*-allyl-N^1-(4-hydroxy salicylaldehyde)-N^4-(salicylaldehyde) isothiosemicarbazide-N,N',O,O'), have been synthesized and characterized by elemental analysis, FT-IR and UV–vis spectroscopy, and molar conductivity. The solid-state structures of the complexes were also determined by single crystal X-ray diffraction. The iron(III) and cobalt(III) complexes adopt distorted square-pyramidal and octahedral geometries, respectively. The strength of the bonding in these complexes was investigated by thermogravimetric studies with both exhibiting stability with complete decomposition not occurring until *ca.* 600 °C.

Keywords: Isothiosemicarbazone; Cobalt complex; Iron complex; TGA; Crystal structure

1. Introduction

S-Alkyl-isothiosemicarbazones are an important class of thiosemicarbazone derivatives since, in spite of different coordination modes with respect to free thiosemicarbazone ligands, much attention has been paid to their synthesis and biological properties such as antimicrobial, antifungal, and antibacterial activities [1–7]. The influence of biological activity is elevated by the condensation of *S*-alkyl-isothiosemicarbazides with aldehydes and ketones such as 2-hydroxybenzaldehyde derivatives [8] that form tridentate NNO donor ligands. These NNO donor ligands can act as either a mono-negative tridentate ligand (by OH deprotonation) or a di-negative tridentate ligand (by OH and NH_2 deprotonation) in coordination with metals [9, 10]. The non-equivalent NH_2 groups of *S*-alkyl-isothiosemicarbazides react with salicylaldehyde and related aromatic aldehydes in the presence of metal ions to form tetradentate N_2O_2 donor ligands which can be regarded as Salen analogs [11].

*Corresponding author. Email: r.takjoo@um.ac.ir

In Salen complexes, the central ion is placed into a planar or nearly planar environment which aids *d* electron delocalization into the N_2O_2 moiety, important for catalytic activity and nonlinear optical properties [12, 13].

In this work, we describe the synthesis of two new Schiff base complexes, chlorido-(*S*-allyl-N^1-(4-hydroxy salicylaldehyde)-N^4-(salicylaldehyde)isothiosemicarbazide-N,N′,O,O′)-iron(III) ethanol solvate (**1**) and the tris(pyridine)-(4-hydroxy salicylaldehyde *S*-allyl-isothiosemicarbazonato-N,N′,O)-cobalt(III) cation isolated as a mixed chloride/bromide salt (**2**), and their characterization by FT-IR and UV–vis spectroscopy, molar conductivity, TGA, and X-ray structure.

2. Experimental

2.1. *Materials and methods*

All solvents and metal salts were of analytical reagent grade and were used without purification. Molar conductivity of the complexes at 10^{-3} M was measured on a Metrohm 712 Conductometer at room temperature. C, H, and N analyzes were obtained using a Thermo Finnigan Flash Elemental Analyzer 1112EA instrument. FT-IR spectra were recorded on a FT-IR 8400-SHIMADZU spectrophotometer, with samples prepared as KBr pellets (500–4000 cm^{-1}). Electronic absorption spectra of compounds were recorded on a SHIMADZU model 2550 UV–vis spectrophotometer. TG analyzes were carried out on a TGA-50 SHIMADZU at a heating rate of 10 °C/min. X-ray single crystal structure determinations were carried out on a Bruker Smart APEX CCD diffractometer.

2.2. *X-Ray crystallography*

Suitable crystals of **1** and **2** were mounted on a Cryoloop® with a film of Paratone® oil, and placed in a cold nitrogen stream on the Bruker-AXS Smart-APEX diffractometer. Full spheres of data were collected using three sets of 400 frames, each of width 0.5° in ω collected at φ = 0.00°, 90.00°, and 180.00° and 2 sets of 800 frames, each of width 0.45° in φ, collected at ω = –30.00 and 210.00° for **1** and three sets of 606 frames (0.3° width in ω) at φ = 0, 120 and 240° for **2**. Analysis of 783 reflections having $I/\sigma(I) > 13$ with *CELL-NOW* [14] showed the crystal of **1** to belong to the triclinic system and to be twinned by a 180° rotation about *a**. Processing of the raw data and generation of final unit cell parameters was performed with *SAINT* [15], while absorption corrections and merging of equivalent reflections were carried out with *TWINABS* [16] for **1** and *SADABS* [17] for **2**. The structures were solved by Patterson methods for **1** and direct methods for **2** (*SHELXS*) [18] and completed by full-matrix, least-squares refinement (*SHELXL*) [18]. The final refinement of **1** employed the full two-component reflection file and all additional computations were carried out with the *SHELXTL* package [19]. Crystallographic details are presented in table 1.

2.3. *Preparation of 2,4-dihydroxybenzaldehyde S-allylisothiosemicarbazone hydrobromide (H_2L)*

H_2L was prepared by following the literature method [20]. Yield: 5.2 g, 85%. m.p.: 190 °C. Anal. Calcd for $C_{11}H_{13}BrN_3O_5S$ (331.21 g mol^{-1}): C, 39.77; H, 4.25; N, 12.65. Found: C,

Table 1. Crystal data for **1** and **2**.

	1	**2**
Formula	$C_{20}H_{21}ClFeN_3O_4S$	$C_{26}H_{26}Br_{0.25}Cl_{0.75}CoN_6O_2S$
F. W.	490.76	592.08
T (K)	100(2)	100(2)
λ (Å)	0.71073	0.71073
Crystal system	Triclinic	Orthorhombic
Space group	*P-1*	$P2_12_12_1$
Unit cell (Å, °)		
a	8.2182(15)	9.892(7)
b	11.862(2)	14.110(9)
c	23.346(5)	18.985(13)
α	79.914(4)	
β	82.089(3)	
γ	80.613(3)	
V (Å^3)	2196.7(7)	2650(3)
Z	4	4
Density (Calcd Mg/m^3)	1.484	1.484
Abs. coeff. (mm^{-1})	0.934	1.215
F (000)	1012	1218
Size (mm)	0.25 × 0.18 × 0.05	0.25 × 0.06 × 0.06
θ range (°)	2.10 to 28.37	1.80 to 27.99
Reflns. total	64,238	22,923
Indep. reflns. (R_{int})	19,876 (0.0511)	6204 (0.0507)
Compl., % to (θ°)	99.5 (28.00)	99.4 (27.75)
T_{max}, T_{min}	0.9548, 0.8000	0.9307, 0.7726
Data/restraints/parameters	19,876/0/544	6204/0/334
GooF on *F*2	1.069	1.040
Final *R*1, w*R*2($I > 2\sigma(I)$)	0.0602, 0.1605	0.0311, 0.0716
*R*1, *wR*2 (all data)	0.0707, 0.1683	0.0341, 0.0738
Largest diff. peak, hole	1.937, −0.822 e.Å^{-3}	0.494, −0.675 e.Å^{-3}

39.56; H, 4.17; N, 12.51%. IR (cm^{-1}): 3250 (ms), 3186 (ms), 3150 (w), 2820–2950 (w), 1650 (w), 1627 (vs), 1581 (vs), 1157 (ms), 1060 (w), 794 (mw). UV–vis (MeOH, λ_{max} nm, log ε, L mol^{-1} cm^{-1}): 240 (4.2), 288sh (4.19), 300 (4.23), 330 (4.46).

2.4. *Preparation of chloro-(S-allyl-N^1-(4-hydroxy salicylaldehyde)-N^4-(salicylaldehyde) isothiosemicarbazide-N,N',O,O')-iron(III) ethanol solvate (1)*

Sodium hydroxide (0.08 g, 2 mM) was added to 2,4-dihydroxybenzaldehyde *S*-allylisothiosemicarbazone hydrobromide (0.33 g, 1 mM) in 10 mL of ethanol. The mixture was stirred for 15 min. Salicylaldehyde (0.146 g, 1.2 mM) was then added to the solution, and the stirring continued for 30 min more followed by the addition of $FeCl_3 \cdot 6H_2O$ (0.27 g, 1 mM) as a solid. The reaction mixture was stirred and heated in a beaker for 1 h at 50 °C. Crystals suitable for X-ray analysis were obtained by slow evaporation of the solution over two weeks at room temperature. Yield: 0.32 g, 65%. m.p.: 213 °C. Anal. Calcd for $C_{20}H_{21}ClFeN_3O_4S$: C, 48.95; H, 4.31; N, 8.56. Found: C, 47.93; H, 4.42; N, 8.48%. IR (cm^{-1}): 3371 (m), 3130 (w), 2970 (w), 2916 (w), 1604 (vs), 1581 (vs), 1535 (vs), 1427 (s), 1365 (m), 1311 (mw), 1283 (vw), 1141 (m), 1041 (w), 987 (w), 918 (w), 840 (w), 802 (w), 763 (m), 685 (m), 610 (mw), 470 (mw). UV–vis [DMF, λ_{max} nm (log ε/M^{-1} cm^{-1})]: 294 (4.51), 404 (4.02), 470 (3.95). Molar conductivity (1.0×10^{-3} M; DMF): 16 Ω^{-1} cm^2 mol^{-1}.

2.5. *Preparation of tris(pyridine)-(4-hydroxy salicylaldehyde S-allylisothiosemicarbazonato-N,N′,O)-cobalt(III) chloride(0.75) bromide(0.25) (2)*

2,4-Dihydroxybenzaldehyde *S*-allyl-isothiosemicarbazonehydrobromide (0.331 g, 0.1 mM) was dissolved in a mixture of 10 mL of absolute ethanol and 2 mL of pyridine. This was stirred for 15 min and the resulting solution was added to a 5 mL ethanolic solution of $CoCl_2{\cdot}6H_2O$ (0.238 g, 0.1 mM). The solution was stirred for 3 h in the beaker at room temperature, during which time the color gradually turned black green. Crystals suitable for X-ray analysis were obtained by slow evaporation of the solution over four days in a refrigerator. Yield: 0.46 g, 76%. m.p.: 195 °C decomposed. Anal. Calcd for $C_{26}H_{26}CoN_6O_2SBr_{0.25}Cl_{0.75}$: C, 52.72; H, 4.24; N, 14.10. Found: C, 52.78; H, 4.17; N, 13.94%. IR (cm^{-1}): 3247 (m), 3109 (s), 3016 (s), 1596 (vs), 1550 (s), 1496 (vs), 1442 (vs), 1357 (s), 1211 (vs), 1160 (s), 1126 (m), 1072 (mw), 1018 (mw), 1001 (w), 933 (mw), 848 (w), 763 (m), 694 (s), 640 (w), 586 (w), 532 (w), 470 (w). UV–vis [MeOH, λ_{max} nm ($\log \varepsilon/M^{-1}$ cm^{-1})]: 250 (4.71), 310 (4.22), 376 (4.26), 556 (2.69). Molar conductivity (1.0×10^{-3} M; DMF): 84 Ω^{-1} cm^2 mol^{-1}.

3. Results and discussion

The two complexes were synthesized in good yields. They have good solubility in DMF and DMSO, but are insoluble in H_2O and $CHCl_3$. C, H, and N analyzes are in good agreement with theoretical values. The molar conductivity of 16 Ω^{-1} cm^2 mol^{-1} for **1** in DMF (10^{-3} M) suggests nonelectrolytic behavior [21] while that of 84 Ω^{-1} cm^2 mol^{-1} for **2** in DMF (10^{-3} M) is consistent with the proposed ionic formulation [22]. The synthetic route is shown in scheme 1. In the preparation of the iron complex, we used slightly more salicylaldehyde to increase the efficiency.

3.1. *Spectral properties*

The IR spectrum of **1** lacks bands assignable to the asymmetric and symmetric stretching modes of the isothioamide NH_2 functional group, indicating that the template reaction had

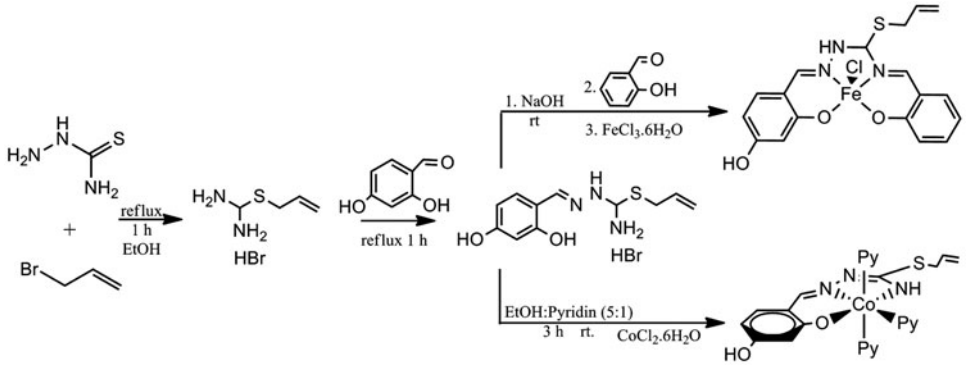

Scheme 1. General synthetic route of complexes.

proceeded to completion [23]. The peak at 3371 cm^{-1} can be assigned to ν(OH) of the lattice ethanol [24] while the very weak bands at 2970–3130 cm^{-1} are due to $\nu(CH)_{aromatic} + \nu(CH_2)_{allyl}$. The complex shows three strong bands at 1604, 1581, and 1535 cm^{-1} which are assigned to ν(C=N) and ν(C=C) combination modes [25]. In addition, the complex exhibits a C–O stretching band at 1141 cm^{-1} that indicates coordination of the deprotonated phenolic oxygen [26]. Bands attributed to N–N stretching and aromatic out-of-plane-bending were found at 1041 and 685 cm^{-1}, respectively. The electronic spectrum of **1** in DMF shows an intra-ligand $n \rightarrow \pi^*$ transition of the isothioamide moiety at 294 nm and LMCT bands for O(p)→M(d) and N(p)→M(d) transitions at 404 and 470 nm, respectively [27]. The tail of the strong LMCT absorption bands may cover the d-d transition bands [28] as the latter could not be located with confidence.

The FT-IR spectrum of **2** shows a sharp band at 3247 cm^{-1} due to stretching vibration of the isothioamide NH group [29]. The asymmetric and symmetric bands of the isothioamide NH_2 group and the ν(OH) band of the phenol were not observed, indicating di-deprotonation of the ligand and coordination to the metal center [22]. The absorption in the 3109–3016 cm^{-1} region can be assigned to the mixture of the C–H pyridine and aromatic stretching vibrations. Four strong bands with the same intensity at 1596, 1505, 1496, and 1442 cm^{-1} are assigned to the combination of $\nu(C{=}N)_{azomethin} + \nu(C{=}N)_{pyridine} + \nu(C{=}C)_{aromatic}$ [30], while a very strong band at 1211 cm^{-1} is assigned to ν(C–O) [31]. The out-of-plane bending vibration modes for the pyridine and aromatic rings are seen at 640 and 694 cm^{-1}, respectively [32]. The electronic spectrum of **2** in methanol exhibits a band at 250 nm attributable to $\pi \rightarrow \pi^*$ transitions of the aromatic ring. The band at 310 nm is assigned to an intra-ligand $n \rightarrow \pi^*$ transition of the isothioamide fragment [20]. A broad band centered at 376 nm is assigned to an LMCT charge transfer transition, while a weak band near 556 nm is attributed to the $^1A_{1g} \rightarrow {}^1T_{1g}$ transition for distorted octahedral cobalt(III) [33].

3.2. *Thermal studies*

Thermo-analytical measurements were performed at 27–1000 °C. The TG curves for **1** and **2** are shown in figure 1 and the proposed mechanisms for thermal decomposition are shown in scheme 2 with theoretical values displayed in parentheses.

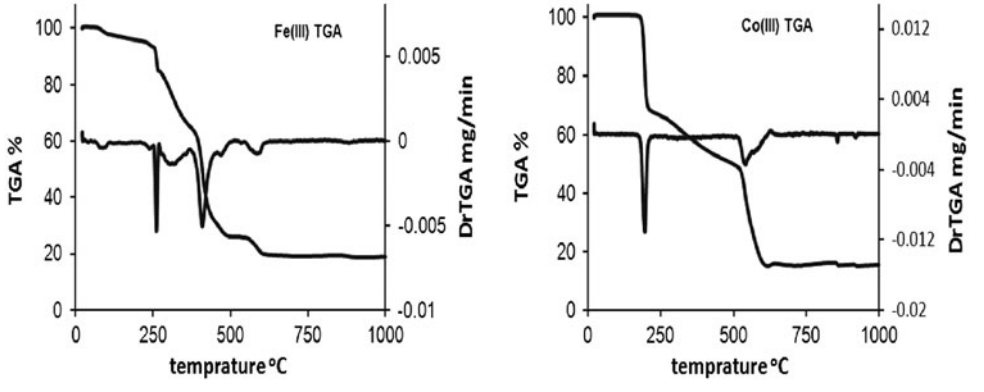

Figure 1. TGA curves of Fe(III) and Co(III) complexes.

The TG curve of **1** showed that the thermal decomposition takes place in five steps. The complex is stable below 87 °C. Gradual decomposition from 87 to 247 °C is related to the loss of the ethanol molecule by an 8.9% weight loss (9.39%). The second step of weight loss, 7% (7.22%), occurs at 260 °C, which is attributed to the separation of a Cl atom. The third stage at 272–360 °C corresponds to a 17.90% (19.96%) weight loss and is attributed to the loss of the *S*-allyl group. The remainder of the ligand is subsequently removed in two stages. From the TG curve, it appears that loss of an N–CH=N–N=C–Ph–(O)OH fragment takes place in the fourth step from 372 to 450 °C with a mass decrease of 35.4% (36.5%), while the last stage, with a 18.77% weight loss (19.50%), corresponds to the loss of a Ph–O fragment at 445–590 °C. The weight of the final product is inconsistent with metal oxide Fe_2O_3 from the 18.36% (17.08%) residual weight.

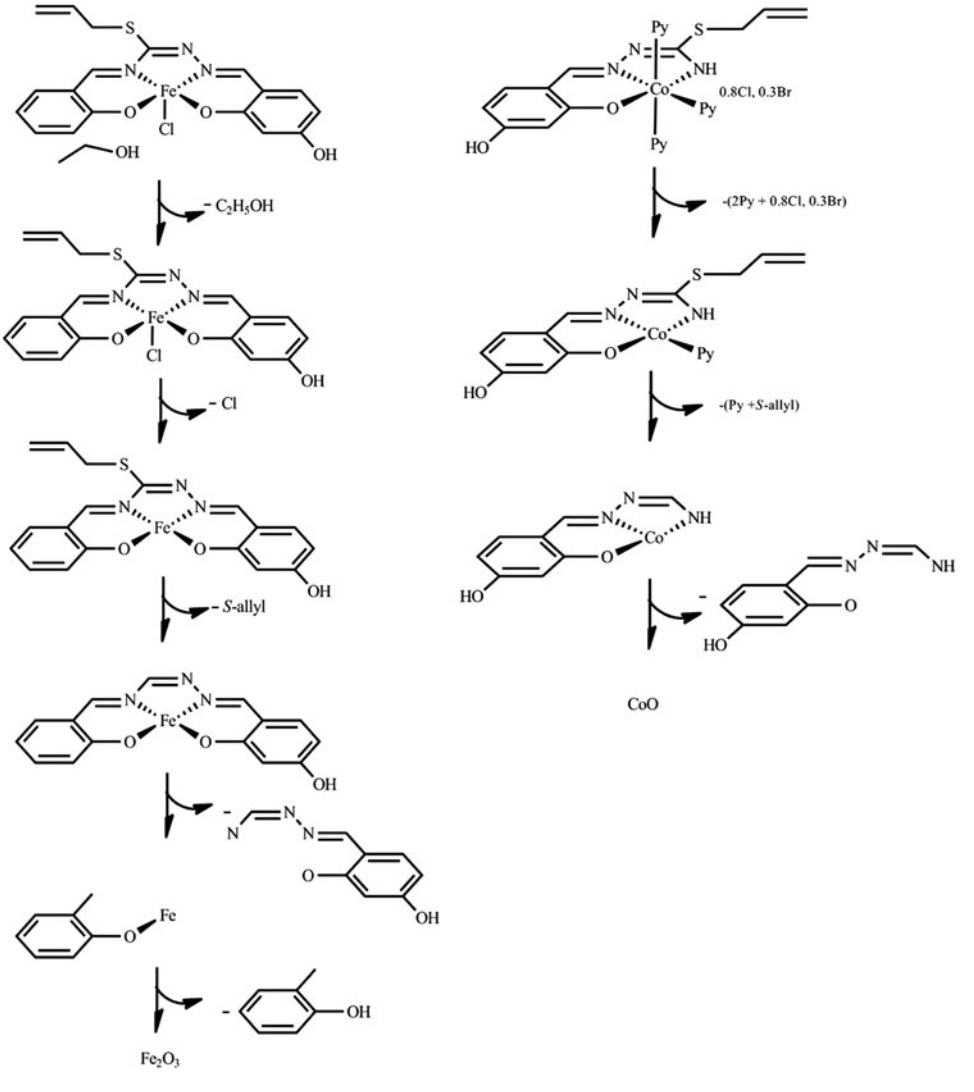

Scheme 2. The proposed mechanisms for thermoanalyses of Fe(III) and Co(III) complexes.

Thermo-analysis of **2** showed that it is generally stable up to 167 °C before the onset of decomposition, which subsequently occurs in three steps. The first step occurs over the range 167–202 °C and corresponds to the loss of two pyridine ligands and the halide ions with a mass loss of 31% (29%). The second stage is a slow process from 202–519 °C due to simultaneous loss of the third pyridine ligand and the *S*-allyl fragment with a mass loss of 22% (22%). The sharp stage with a mass loss of 33% (31%) corresponds to the removal of the NH–C=N–N=C–Ph–(O)(OH) fragment. The final decomposition product is cobalt oxide as indicated by the residual weight of 15% (13%).

3.3. *Crystal structures*

Pertinent bond distances and interbond angles for **1** and **2** are presented in tables 2 and 5, respectively, while perspective views of the complexes are shown in figures 2 and 3, respectively. There are also some hydrogen bonds in complexes 1 and 2 that are shown in table 3 and 6, respectively. From table 2, the corresponding metal–ligand bond distances in the two independent molecules are substantially the same, while the corresponding angles tend to differ to a greater extent. This is also evident from table 4, which shows that each of the three chelate rings formed by the tetradentate ligand are more folded along the line joining the respective donor atoms in molecule **2** than in molecule **1**. Despite this, the distance of the iron atom from the mean plane of the four donor atoms is the same in both (0.534(1) and 0.536(1) Å). The coordination geometry can thus be described as distorted square-pyramidal (SPY) with the metal atom displaced from the basal plane towards the apical ligand.

A five-coordinate complex can adapt a trigonal–bipyramidal (TBPY) or SPY geometry. Addison *et al.* introduced the parameter τ that is used for determining TBPY or SPY configuration. The parameter τ is defined as $\tau = (\beta - \alpha)/60$ (where β and α are the largest angles in the metal coordination sphere with $\beta > \alpha$). This value for **1** is 0.06, indicating that the complex has a slightly distorted SPY geometry [34].

The Fe–O and Fe–N bond lengths are similar to those reported in the crystal structures of SPY coordinated Fe(III) complexes with N_2O_2 donor isothiosemicarbazone derivatives [21]. Coordination of the asymmetric ligand to the iron atom generates three chelate rings, two six-membered and one five-membered. In the isothioamide fragment, the C–C and C=N

Table 2. Bond distances (Å) and interbond angles (°) for **1**.

Molecule 1		Molecule 2	
Fe1–O2	1.898(2)	Fe2–O5	1.894(2)
Fe1–O1	1.9090(19)	Fe2–O4	1.901(2)
Fe1–N1	2.068(2)	Fe2–N4	2.059(2)
Fe1–N3	2.099(2)	Fe2–N6	2.094(2)
Fe1–Cl1	2.2532(8)	Fe2–Cl2	2.2440(8)
O2–Fe1–O1	95.68(8)	O5–Fe2–O4	94.06(8)
O2–Fe1–N1	144.47(9)	O5–Fe2–N4	146.41(10)
O1–Fe1–N1	86.99(9)	O4–Fe2–N4	87.39(9)
O2–Fe1–N3	86.58(9)	O5–Fe2–N6	86.87(9)
O1–Fe1–N3	148.77(9)	O4–Fe2–N6	147.34(10)
N1–Fe1–N3	73.97(9)	N4–Fe2–N6	74.68(10)
O2–Fe1–Cl1	107.32(7)	O5–Fe2–Cl2	110.80(7)
O1–Fe1–Cl1	106.85(7)	O4–Fe2–Cl2	110.51(7)
N1–Fe1–Cl1	105.70(7)	N4–Fe2–Cl2	99.93(7)
N3–Fe1–Cl1	102.10(7)	N6–Fe2–Cl2	99.49(7)

Table 3. Hydrogen bonds for **1** (Å and °).

D–H···A	d(D–H)	d(H···A)	d(D···A)	∠(DHA)
O8–H8O···O4[i]	0.95	1.92	2.831(3)	159
O7–H7O···O1	0.88	1.93	2.745(3)	154
O6–H6O···O7	0.92	1.70	2.613(3)	169
O3–H3O···O8[ii]	0.88	1.75	2.622(3)	170

Note: Symmetry transformations used to generate equivalent atoms: [i]*x*, *y* + 1, *z*; [ii]*x*, *y*–1, *z*.

Table 4. Chelate ring folding (°) for **1**.

		Molecule 1	Molecule 2
Fold along line	O1–N1	10.5(2)	
	O4–N4		16.2(2)
	N1–N3	14.2(2)	
	N4–N6		17.4(2)
	O2–N3	20.0(1)	
	O5–N6		26.4(2)

bond distances have classical single and double bond characters, indicating π-delocalization of electron density over this moiety.

In the X-ray sample, the Co(III) complex cation in **2** was isolated as a mixed chloride/bromide salt in a 3/1 ratio. From table 5, the coordination geometry is that of a modestly

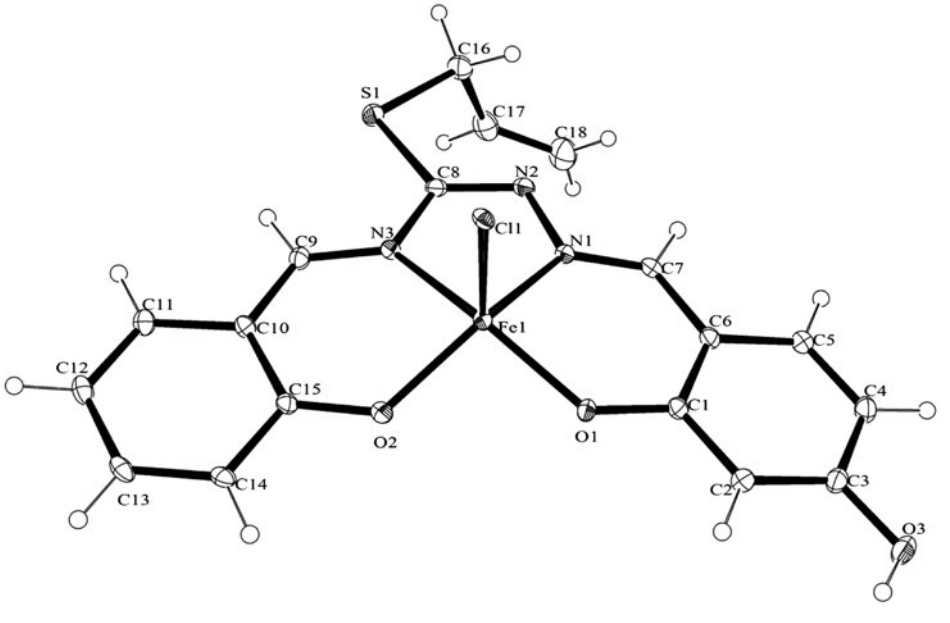

Figure 2. Perspective view of molecule 1 of **1**. Displacement ellipsoids are drawn at the 50% probability level and hydrogens are drawn as spheres of arbitrary radius.

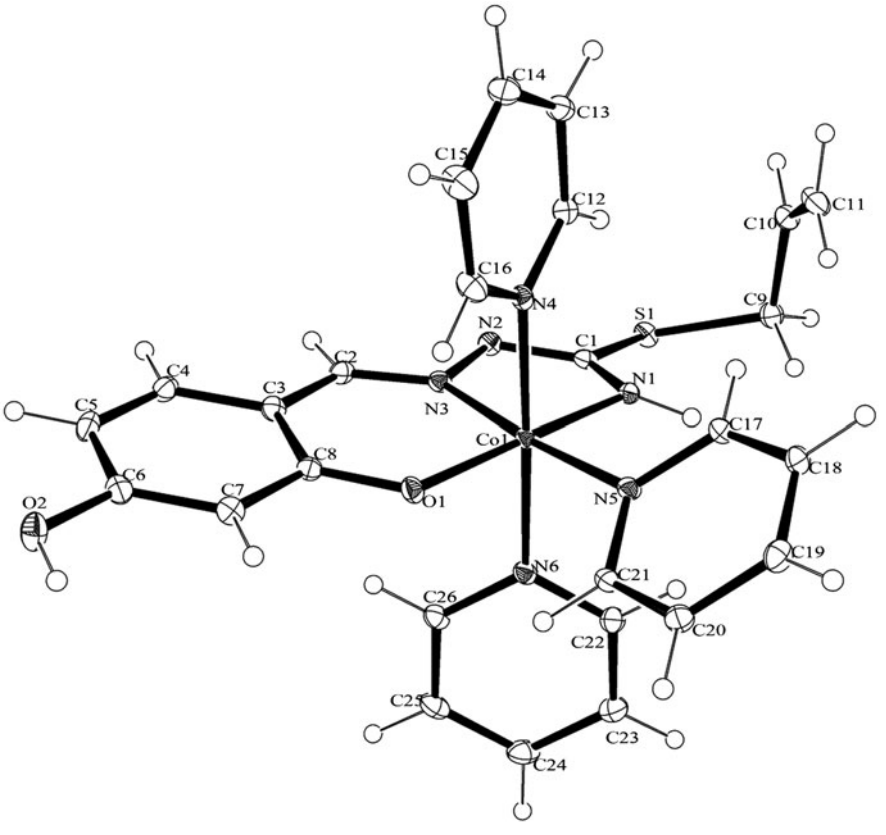

Figure 3. Perspective view of the cation of **2**. Displacement ellipsoids are drawn at the 50% probability level and hydrogens are drawn as spheres of arbitrary radius.

distorted octahedron, with the largest deviations from the ideal resulting from the constraints of the Schiff base ligand. That ligand is nearly planar but with a slight twist from end to end.

The dibasic tridentate ligand coordinated to the metal center via the isothioamide nitrogen, azomethine nitrogen, and phenolic oxygen atoms. Remaining sites of the octahedral geometry are occupied with three pyridine molecules. N1 and N3 atoms are in *cis* position

Table 5. Bond distances (Å) and interbond angles (°) for **2**.

Co1–N3	1.882(2)	Co1–N5	1.959(2)
Co1–O1	1.8882(18)	Co1–N6	1.975(2)
Co1–N1	1.907(2)	Co1–N4	1.990(2)
N3–Co1–O1	94.96(9)	N1–Co1–N6	89.18(8)
N3–Co1–N1	82.13(9)	N5–Co1–N6	92.50(8)
O1–Co1–N1	175.67(8)	N3–Co1–N4	88.70(9)
N3–Co1–N5	174.85(8)	O1–Co1–N4	89.98(8)
O1–Co1–N5	88.34(9)	N1–Co1–N4	93.15(8)
N1–Co1–N5	94.80(9)	N5–Co1–N4	87.34(9)
N3–Co1–N6	91.59(9)	N6–Co1–N4	177.67(8)
O1–Co1–N6	87.69(8)	N1–Co1–N6	89.18(8)

Table 6. Hydrogen bonds for **2** (Å and °).

D–H···A	d(D–H)	d(H···A)	d(D···A)	∠(DHA)
O2–H1···Cl1	0.84	2.25	3.075(2)	165
N1–H1 N···Cl1^{i}	0.88	2.59	3.452(3)	168

Note: Symmetry transformations used to generate equivalent atoms: $^{i}-x+2, y+1/2, -z+1/2$.

with respect to each other, confirming the ligand coordinates to the cobalt in the *E* form [30].

The observed Co–N1 (1.907(2) Å), Co–N3 (1.882(2) Å), and Co–O1 (1.888(2) Å) distances agree well with previously reported values [35]. The average Co–N (nitrogen of pyridine molecules) distance (1.974(6) Å) is similar to the reported values [35]. The bond distances in isothioamide fragment show that π electron delocalization exists in the deprotonated coordinated organic ligand.

The angle between two chelate rings is 4.41°, showing the ligand coordinates to the metal in a concave form. The pyridine molecules are bent off the N1–N3–O1–N5 plane by 37.25–89.84°. The bond angles around the central ion are from 87.3(8) to 94.8(8)°. The bite angles O1–Co1–N1 and N3–Co1–N5 are 175.67(8)° and 174.85(8)°, respectively, matching the values from the literature for other Co(III) complexes of isothiosemicabazone [36].

4. Conclusion

Treatment of Co(II) chloride in a mixture of ethanol and pyridine with *S*-allyl-isothiosemicarbazone hydrobromide ($H_2L{\cdot}HBr$) gave $[Co(L^1)(Py)_3]{\cdot}Cl_{0.75}Br_{0.25}$, where L^1=4-hydroxy salicylaldehyde *S*-allyl-isothiosemicarbazonato-N,N′,O) as a N_2O donor ligand. Likewise, the template reaction of 2,4-dihydroxybenzaldehyde *S*-allyl-isothiosemicarbazone hydrobromide with salicylaldehyde in the presence of iron(III) chloride and NaOH yielded $[Fe(L^2)Cl]{\cdot}C_2H_5OH$, where L^2=*S*-allyl-N^1-(4-hydroxy salicylaldehyde)-N^4-(salicylaldehyde) isothiosemicarbazide-N,N′,O,O′) as a N_2O_2 donor ligand. The complexes were characterized by elemental analysis, IR and UV–vis spectra, and X-ray crystal structure determinations. In $[Fe(L)Cl]{\cdot}C_2H_5OH$, Fe(III) had a SPY configuration with the N_2O_2 donor in the basal positions and the apical position occupied by the chloride. Co(III) in $[Co(L)(Py)_3]{\cdot}Cl_{0.75}Br_{0.25}$ is approximately octahedral with the Schiff base tridentate coordinating via azomethine nitrogen, deprotonated thioamide nitrogen, and the deprotonated phenoxy; three pyridines occupy the remaining positions. Thermal stabilities of the cobalt(III) and iron(III) complexes were also studied and discussed. The TG curves displayed three and five steps of thermal decomposition for the Co(III) and Fe(III) complexes, respectively.

Supplementary material

CCDC 890227-890228 contain the supplementary crystallographic data for **1** and **2**. These data can be obtained free of charge via http://www.ccdc.cam.ac.uk/conts/retrieving.html, or

from the Cambridge Crystallographic Data Center, 12 Union Road, Cambridge CB2 1EZ, UK; Fax: (+44) 1223-336-033; or E-mail: deposit@ccdc.cam.ac.uk.

Acknowledgments

The authors thank the Tulane University Chemistry Department for support of the Tulane Crystallography Laboratory. R. T. and A. A. thank Ferdowsi University of Mashhad and Payame Noor University (PNU) for financial assistance.

References

[1] M.T. Cocco, C. Congiu, V. Onnis, M.L. Pelleranob, A.D. Logu. *Bioorg. Med. Chem.*, **10**, 501 (2002).
[2] A. Plumitallo, M.C. Cardia, S. Distinto, A.D. Logu, E. Maccioni. *IL Farmaco*, **59**, 945 (2004).
[3] A.D. Logua, M. Saddi, V. Onnis, C. Sanna, C. Congiu, R. Borgna, M.T. Cocco. *Int. J. Antimicrob. Agents*, **26**, 28 (2005).
[4] E. Maccioni, M.C. Cardia, L. Bonsignore, A. Plumitallo, M.L. Pellerano, A.D. Logu. *IL Farmaco*, **57**, 809 (2002).
[5] R. Yanardag, T.B. Demirci, B. Ülküseven, S. Bolkent, S. Tunali, S. Bolkent. *Eur. J. Med. Chem.*, **44**, 818 (2009).
[6] T. Bal, B. Atasever, Z. Solakoğlu, S. Erdem-Kuruca, B. Ülküseven. *Eur. J. Med. Chem.*, **42**, 161 (2007).
[7] E. Maccioni, M.C. Cardia, S. Distinto, L. Bonsignore, A.D. Logu. *IL Farmaco*, **58**, 951 (2003).
[8] S. E-Öztürk, T. Karayildirim, H. Anil. *Bioorg. Med. Chem.*, **19**, 1179 (2011).
[9] M.V. Rodić, V.M. Leovac, L.S. Jovanović, L.S. Vojinović-Ješić, V. Divjaković, V.I. Češljević. *Polyhedron*, **46**, 124 (2012).
[10] V. Jevtovic, D. Vidovic. *J. Chem. Crystallogr.*, **40**, 794 (2010).
[11] V.B. Arion, P. Rapta, J. Telser, S.S. Shova, M. Breza, K. Luspai, J. Kozisek. *Inorg. Chem.*, **50**, 2918 (2011).
[12] J. Zhang, C. Zhong, X. Zhu, H.-L. Tam, K.-F. Li, K.-W. Cheah, W.-Y. Wong, W.-K. Wong, R.A. Jones. *Polyhedron*, **49**, 121 (2013).
[13] P. Sudheesh, K. Chandrasekharan. *Solid State Commun.*, **152**, 268 (2012).
[14] G.M. Sheldrick. *CELL-NOW*, University of Göttingen, Germany (2008).
[15] Bruker-AXS. *SAINT (Version 7.68A)*, Madison, WI (2009).
[16] G.M. Sheldrick. *TWINABS*, University of Göttingen, Germany (2008).
[17] G.M. Sheldrick. *SADABS (Version 2008/2)*, University of Göttingen, Germany (2008).
[18] G.M. Sheldrick. *SHELXS and SHELXL. Acta Cryst. A*, **64**, 112 (2008).
[19] Bruker-AXS. *SHELXTL (Version 2008/4)*, Madison, WI (2008).
[20] R. Takjoo, J.T. Mague, A. Akbari, M. Ahmadi. *J. Coord. Chem.*, **66**, 1854 (2013).
[21] M. Ahmadi, J.T. Mague, A. Akbari, R. Takjoo. *Polyhedron*, **42**, 128 (2012).
[22] B. Atasever, B. Ulkuseven, T.B. Demirci, S.E. Kuruca, Z. Solakoglu. *Invest. New Drugs*, **28**, 421 (2010).
[23] K. Nakamoto. *Infrared and Raman Spectra of Inorganic and Coordination Compounds: Theory and Applications in Inorganic Chemistry, Part-A*, 5th Edn, p. 11., Wiley Inc., New York, NY (1997).
[24] H. Hosseini Monfared, S. Alavi, R. Bikas, M. Vahedpour, P. Mayer. *Polyhedron*, **29**, 3355 (2010).
[25] (a) A. Akbari, M. Ahmadi, R. Takjoo, F.W. Heinemann. *J. Coord. Chem.*, **65**, 4115 (2012); (b) A. Akbari, M. Ahmadi, R. Takjoo, F.W. Heinemann, *J. Coord. Chem.*, **66**, 1886 (2013).
[26] V.B. Arion, V.C. Kravtsov, R. Goddard, E. Bill, J.I. Gradinaru, N.V. Gerbeleu, V. Levitschi, H. Vezin, Y.A. Simonov, J. Lipkowski, V.K. Belskii. *Inorg. Chim. Acta*, **317**, 33 (2001).
[27] B. Turkkan, B. Sarıbog, N. Sarıbog. *Transition Met. Chem.*, **36**, 679 (2011).
[28] A. Kumar, R. Borthakur, A. Koch, O.B. Chanu, S. Choudhury, A. Lemtur, R.A. Lal. *J. Mol. Struct.*, **999**, 89 (2011).
[29] K.Y. Choi, S.M. Yang, K.C. Lee, H. Ryu, C.H. Lee, J. Seo, M. Suh. *Transition Met. Chem.*, **33**, 99 (2008).
[30] (a) R. Takjoo, A. Akbari, M. Ahmadi, H. Amiri Rudbari, G. Bruno. *Polyhedron*, **55**, 225 (2013); (b) R. Takjoo, M. Ahmadi, A. Akbari, H. Amiri Rudbari, F. Nicoloi, *J. Coord. Chem.*, **65**, 3403 (2012).
[31] M. Shebl. *Spectrochim. Acta, Part A*, **70**, 850 (2008).
[32] R. Takjoo, R. Centore, M. Hakimi, S.A. Beyramabadi, A. Morsali. *Inorg. Chim. Acta*, **371**, 36 (2011).
[33] A. Ray, G.M. Rosair, R. Kadam, S. Mitra. *Polyhedron*, **28**, 769 (2008).
[34] A.W. Addison, T.N. Rao, J. Reedjik, J. Van Rijn, G.C. Verschoor. *Dalton Trans.*, 1349 (1984).
[35] S.B. Novaković, G.A. Bogdanović, V.M. Leovac. *Polyhedron*, **25**, 1096 (2006).
[36] G.A. Bogdanovic, V.B. Medakovic, L.S. Vojinovic, V.I. Cesljevic, V.M. Leovac, A.S. de Bire, S.D. Zaric. *Polyhedron*, **20**, 2231 (2001).